

# Convexity-based Camouflage Breaking

Ariel Tankus                      Yehezkel Yeshurun  
Department of Computer Science  
Tel-Aviv University  
Tel-Aviv 69978, Israel  
{arielt,hezy}@math.tau.ac.il

## Abstract

*This paper presents biological evidence for camouflage breaking using the convexity of the intensity function. Some animals use apatetic coloring especially to prevent their detection by graylevel convexity. This implies that other animals might be able to break camouflage based on graylevel convexity. We demonstrate the effectiveness of convexity based camouflage breaking using an operator (“ $D_{arg}$ ”) for detection of 3D convex or concave graylevels. Its high robustness and the biological motivation make  $D_{arg}$  particularly suitable for camouflage breaking. As will be demonstrated, the operator is able to break very strong camouflage, which might delude even human viewers. Being non-edge-based, the performance of the operator is juxtaposed with that of a representative edge-based operator in the task of camouflage breaking. Better performance is achieved by  $D_{arg}$  for animal as well as military camouflage breaking.*

## 1. Introduction

“Camouflage is an attempt to obscure the signature of a target and also to match its background” [1]. Work related to camouflage can be roughly divided into two: camouflage assessment and design (e.g, [1], [2]), and camouflage breaking. Despite the ongoing research, only little has been said in the computer vision literature on visual camouflage breaking: [5], [10], [4], [3].

In this paper, we address the issue of *visual camouflage breaking*. We present biological evidence that graylevel convexity may break camouflage. This is based on Thayer’s principle of counter-shading [11], which observes that some animals use apatetic coloration to prevent their image (under sun light) from appearing as convex graylevels to a viewer. This implies that other animals may be able to break camouflage based on convexity of the graylevels they see (or else there was no need in such an apatetic coloration).

Our goal is therefore to detect 3D convex or concave objects under strong camouflage. For this task, we employ the

suggested operator (“ $D_{arg}$ ”), which is applied directly to the intensity function.  $D_{arg}$  is based on the 3D structure of objects, and responds to smooth 3D convex or concave domains. The operator is not limited to any particular light source or reflectance function. It does not attempt to restore the 3D scene. The purpose of the operator is *detection* of convex or concave objects in highly cluttered scenes, and in particular under camouflage conditions.

The robustness and invariance characterizing  $D_{arg}$  (see [9]) as well as the biological motivation make it suitable for camouflage breaking, even for camouflages that might delude a human viewer. In contrast with existing attempts to break camouflage, our operator is context-free; its only a priori assumption about the target is its being 3D and convex (or concave). In order to evaluate the performance of the operator in breaking camouflage, we juxtaposed  $D_{arg}$  with a representative edge-based operator. Only a small portion of the comparison can fit into this paper.

The next section defines the convexity-based operator  $D_{arg}$ . Section 2.1 gives intuition for  $D_{arg}$  and is of particular importance for understanding its behavior. Section 3 utilizes  $D_{arg}$  for camouflage breaking. Section 3.1 brings the biological evidence for camouflage breaking by graylevel convexity. Section 3.2 delineates a camouflage breaking comparison of an edge-based method with our convexity-based operator. Concluding remarks are in section 4.

## 2. $Y_{arg}$ , $D_{arg}$ : Operators for Detection of Convex Domains

We next define an operator for detection of three dimensional objects with smooth convex or concave domains.

Let  $I(x, y)$  be an input image, and  $\nabla I(x, y) = (\frac{\partial}{\partial y}I(x, y), \frac{\partial}{\partial x}I(x, y))$  the Cartesian representation of the gradient map of  $I(x, y)$ . Let us convert  $\nabla I(x, y)$  into its *polar* representation. The gradient argument is defined by:

$$\theta(x, y) = \arg(\nabla I(x, y)) = \arctan \left( \frac{\partial}{\partial y}I(x, y) , \frac{\partial}{\partial x}I(x, y) \right)$$

where the two dimensional arc tangent is:

$$\arctan(y, x) = \begin{cases} \arctan(\frac{y}{x}), & \text{if } x \geq 0 \\ \arctan(\frac{y}{x}) + \pi, & \text{if } x < 0, y \geq 0 \\ \arctan(\frac{y}{x}) - \pi, & \text{if } x < 0, y < 0 \end{cases}$$

and the one dimensional  $\arctan(t)$  denotes the inverse function of  $\tan(t)$  so that:  $\arctan(t) : [-\infty, \infty] \mapsto [-\frac{\pi}{2}, \frac{\pi}{2}]$ .

The proposed convexity mechanism, which we denote:  $Y_{arg}$ , is simply the  $y$ -derivative of the argument map:

$$Y_{arg} = \frac{\partial}{\partial y} \theta(x, y) = \frac{\partial}{\partial y} \arctan \left( \frac{\partial}{\partial y} I(x, y), \frac{\partial}{\partial x} I(x, y) \right)$$

To obtain an isotropic operator based on  $Y_{arg}$ , we rotate the original image by  $0^\circ, 90^\circ, 180^\circ$  and  $270^\circ$ , operate  $Y_{arg}$ , and rotate the results back to their original positions. The sum of the four responses is the response of an operator which we name:  $D_{arg}$ .

## 2.1. Intuition for $Y_{arg}$

### • What Does $Y_{arg}$ Detect?

$Y_{arg}$  detects the zero-crossings of the gradient argument. This stems from the last step of the gradient argument calculation: the two-dimensional arc-tangent function. The arc-tangent function is discontinuous at the negative part of the  $x$ -axis; therefore its  $y$ -derivative approaches infinity there. In other words,  $Y_{arg}$  approaches infinity at the negative part of the  $x$ -axis of the arctan, when this axis is being crossed. This infinite limit reveals the zero-crossings of the gradient argument! (see [9] for more details).

### • Why Detect Zero-Crossings of Gradient Argument?

$Y_{arg}$  detects zero-crossings of the gradient argument of the intensity function  $I(x, y)$ . The existence of zero-crossings of the gradient argument enforces a certain range of values on the gradient argument (values which are typical near  $x = 0, y < 0$ ). Considering the intensity function  $I(x, y)$  as a surface in  $R^3$ , the gradient argument “represents” the direction of the normal to the surface. Therefore, a range of values of the gradient argument means a certain range of directions of the normal to the intensity surface. This enforces a certain structure on the intensity surface itself.

In [9] we have characterized the structure of the intensity surface as either a paraboloidal structure or any derivable strongly monotonically increasing transformation of a paraboloidal structure (Fig. 1). Since paraboloids are arbitrarily curved surfaces, they can be used as a local approximation of 3D convex or concave surfaces (Recall, that our input is discrete, and the continuous functions are only an approximation!). The detected intensity surface domains

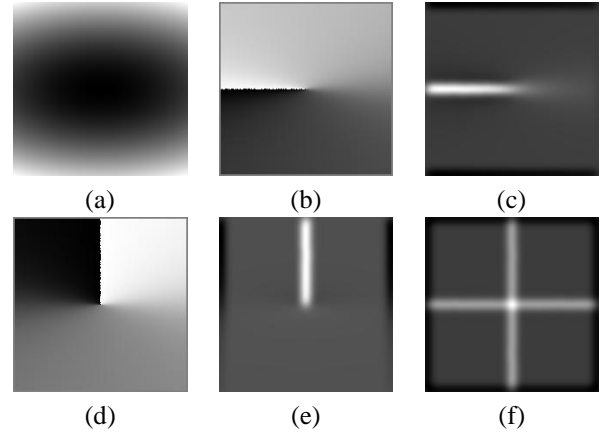


**Figure 1.** (a) Paraboloidal graylevels:  $I(x, y) = 10x^2 + 40y^2$ . (b) Gradient argument of (a). Discontinuity ray at negative  $x$ -axis. (c)  $Y_{arg}$  of (a) ( $= \frac{\partial}{\partial y}$  of (b)). (d) Rotate (a)  $90^\circ$  c.c.w, calculate gradient argument, and inverse rotate. (e) Rotate (a)  $90^\circ$  c.c.w, calculate  $Y_{arg}$ , and inverse rotate. (f)  $D_{arg}$ , the isotropic operator.

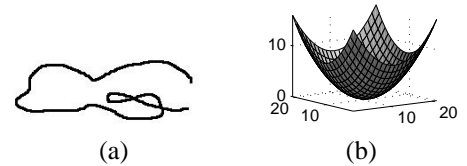


**Figure 2.** 3D vs. 2D convexity. (a) 2D convexity: A contour is a 1D surface in  $R^2$ . (b) 3D convexity: A paraboloid is a 2D surface in  $R^3$ .

are therefore those exhibiting 3D convex or concave structure. The convexity is three dimensional, because this is the convexity of the intensity surface  $I(x, y)$  ( $= 2D$  surface in  $R^3$ ; Fig. 2(b)), and *not* convexity of contours ( $= 1D$  surface in  $R^2$ ; Fig. 2(a)). This 3D convexity of the intensity surface is characteristic of intensity surfaces emanating from smooth 3D convex bodies.

### • Intuition Summary

One may detect the zero-crossings of the gradient argument by detecting the infinite response of  $Y_{arg}$  at the negative  $x$ -axis (of the arctan). These zero-crossings occur where the intensity surface is 3D convex or concave. Convex smooth 3D objects usually produce 3D convex intensity surfaces. Thus, detection of the infinite responses of  $Y_{arg}$  results in detection of domains of the intensity surface which characterize 3D smooth convex or concave subjects.

## 3. Camouflage Breaking

The robustness of the operator under various conditions (illumination, scale, orientation, texture) has been thor-

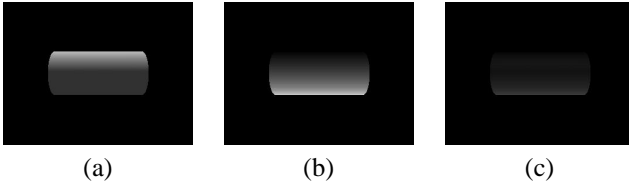


**Figure 3. Thayer’s principle of counter shading.** (a) A cylinder of constant albedo under top lighting. (b) A counter-shaded cylinder under ambient lighting. (c) Thayer’s principle: the combined effect of counter-shading albedo and top lighting breaks up the shadow effect (= convex intensity function).

oughly studied in [9]. As a result, the smoothness condition of the detected 3D convex objects can be relaxed. In this paper, we further increase the robustness demands from the operator by introducing very strong camouflage.

### 3.1. Biological Evidence for Camouflage Breaking by Convexity

Next, we exhibit evidence of biological camouflage breaking based on the convexity of the intensity function. This matches our idea of camouflage breaking by convexity detection (using  $D_{arg}$ ). We bring further evidence, that not only can intensity convexity break camouflage, but also there are animals whose coloring is suited to prevent this specific technique of camouflage breaking.

It is well known that under directional light, a smooth 3D convex object produces a convex intensity function. The biological meaning is that when the trunk of an animal (the convex subject) is exposed to top lighting (sun), a viewer sees shades (convex intensity function). As we shall see, these shades may reveal the animal, especially in surroundings which break up shadows (e.g., woods) (see [7]). This biological evidence supports  $D_{arg}$ ’s modus operandi of camouflage breaking by detecting convexity of the intensity function.

The ability to trace an animal based on these shadow effects has led, during thousands of years of evolution, to coloration of animals that dissolves the shadow effects. This counter-shading coloration was first observed at the beginning of the previous century [11], and is known as Thayer’s principle. Portmann [7] describes Thayer’s principle: “If we paint a cylinder or sphere in graded tints of gray, the darkest part facing toward the source light, and the lightest away from it, the body’s own shade so balances this color scheme that the outlines becomes dissolved. Such graded tints are typical of vertebrates and of many other animals.” Figure 3 uses ray tracing to demonstrate Thayer’s principle of counter-shading when applied to cylinders. The sketches in Fig. 4, taken from [7], demonstrate how animal coloration changes gradually from dark (the upper part) to

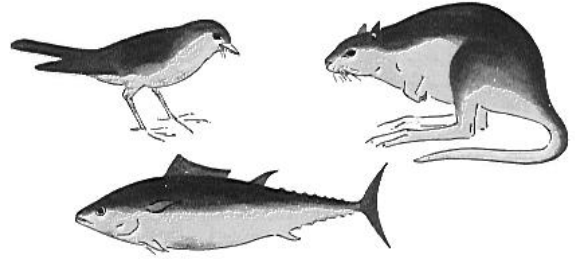


**Figure 4. Thayer’s principle.** The animal’s upper part is darker; albedo changes gradually towards bright in the lower part. When the animal is in sun light, this coloration breaks the convexity of the intensity function.

bright (the lower part). When the animal is under top lighting (sun light), the gradual change of albedo neutralizes the convexity of the intensity function. Had no counter-shading been used, the intensity function would have been convex (as in Fig. 3(a)), exposing the animal to convexity based detectors (such as  $D_{arg}$ ). Putting counter-shading into effect neutralizes the convexity of the intensity function thus disabling convexity-based detection.

The existence of counter-measures to convexity based detectors implies that there might exist predators who use convexity based detectors similar to  $D_{arg}$ .

### 3.2. Experimental Results

In this section we juxtapose  $D_{arg}$  with a typical edge-based operator—radial symmetry transform [8]—as camouflage breakers. This operator seeks generalized symmetry, and has been shown there to generalize several edge-based operators. We compare  $D_{arg}$  with edge-based methods, since camouflage by super-excitation of a predator’s edge detectors is evident in the animal kingdom [6] (implying edges are used biologically for camouflage breaking).

#### 3.2.1 Apatetic Coloration in Animals

Animals use various types of camouflage to hide themselves, one of which is apatetic coloration. Fig. 5 exhibits a natural camouflage of a squirrel in a leafy environment under the shades of a nearby tree. The camouflaged fur has many edges which mix with the environment, preventing the radial symmetry operator from isolating any specific target.  $D_{arg}$ , however, produces a single strong peak, exactly on the squirrel. The convexity of the squirrel (and in particular, its belly) is the reason for its detection by  $D_{arg}$ . The only smooth 3D convex region in the image is the belly of the squirrel. Though some of the shades might look similar to a belly of a squirrel (even to a human viewer), they do not possess the property of being a projection of a 3D convex object, so their graylevels introduce no 3D convexity.

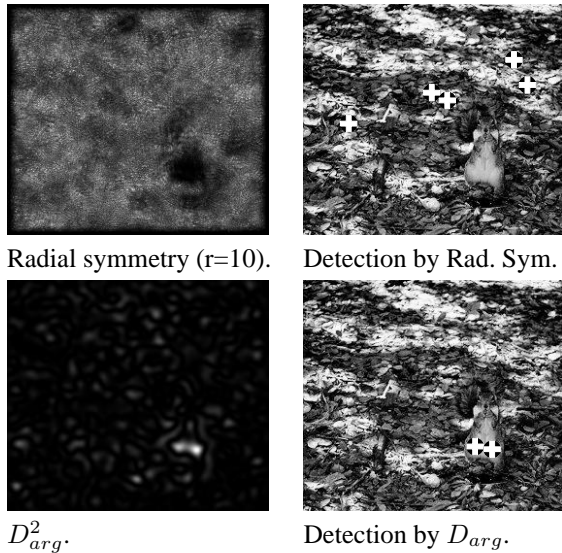


**Figure 5. A hidden squirrel: a squirrel on a leafy ground shaded by a tree. The shades and leaves form many edges “deluding” edge-based methods. Even human viewers find it difficult to locate the squirrel in the image.  $D_{arg}$  detects the squirrel, breaking the camouflage.**

### 3.2.2 Military Camouflage

Breaking camouflage of equipment is of particular interest. Figure 6 presents tanks in a highly cluttered scene. The edges of the urban area distract edge-based detectors. The convexity of the tanks leads to detection of 2 out of 3 tanks by  $D_{arg}$  (the third tank is too small to detect).

## 4. Conclusions

We have shown biological motivation for camouflage breaking using convexity: Thayer’s principle states that various animals use counter-shading to prevent camouflage breaking by intensity function convexity. The observation of such a counter-measure in animals implies that other animals might use convexity to break camouflage (or otherwise there was no need in the counter-measure). The effectiveness of camouflage breaking by convexity is demonstrated using  $D_{arg}$ . The operator  $D_{arg}$  is basically intended for detection of image domains emanating from smooth convex or concave 3D objects, but the smoothness assumption can be relaxed. The mathematical basis for the robustness of  $D_{arg}$  had been given in [9]. Finally, a comparison has been delineated between the convexity-based camouflage breaker ( $D_{arg}$ ) and an edge-based operator (radial symmetry). Convexity-based camouflage breaking was found very robust and in many cases much more effective than edge-based techniques.

• Supported by grants from: Minerva Minkowski center for

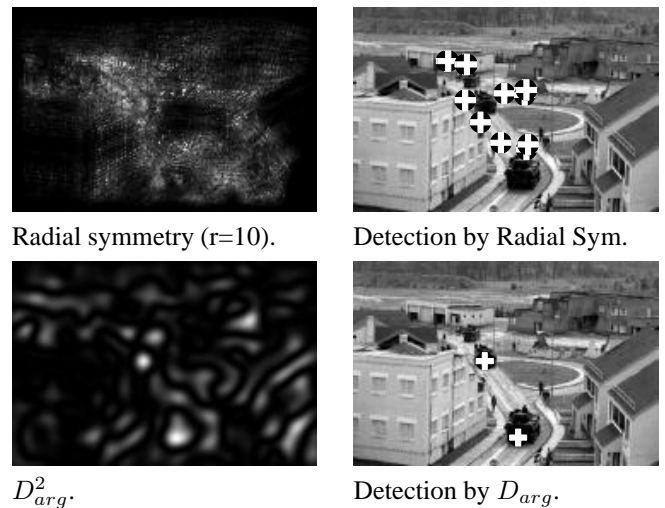


**Figure 6. Tanks in an urban zone (i.e., high clutter). Edge-based detection is distracted by the background. Convexity-based  $D_{arg}$  detects 2 of the 3 tanks.**

geometry, Israel Academy of Science for Geometric Computing, and the Moscona fund.

## References

- [1] A. C. Copeland and M. M. Trivedi. Models and metrics for signature strength evaluation of camouflaged targets. *Proceedings of the SPIE*, 3070:194–199, 1997.
- [2] F. M. Gretzmacher, G. S. Ruppert, and S. Nyberg. Camouflage assessment considering human perception data. *Proceedings of the SPIE*, 3375:58–67, 1998.
- [3] S. Guilan and T. Shunqing. Method for spectral pattern recognition of color camouflage. *Optical Engineering*, 36(6):1779–1781, June 1997.
- [4] S. Marouani, A. Huertas, and G. Medioni. Model-based aircraft recognition in perspective aerial imagery. In *Proc. of the Intl. Symp. on Comp. Vision*, pages 371–376, USA, 1995.
- [5] S. P. McKee, S. N. J. Watamaniuk, J. M. Harris, H. S. Smallman, and D. G. Taylor. Is stereopsis effective in breaking camouflage? *Vision Research*, 37:2047–2055, 1997.
- [6] D. Osorio and M. V. Srinivasan. Camouflage by edge enhancement in animal coloration patterns and its implications for visual mechanisms. *Proceedings of the Royal Society of London B*, 244:81–85, 1991.
- [7] A. Portmann. *Animal Camouflage*, pages 30–35. The University of Michigan Press, 1959.
- [8] D. Reisfeld, H. Wolfson, and Y. Yeshurun. Context free attentional operators: the generalized symmetry transform. *Intl. Journal of Computer Vision*, pages 119–130, 1995.
- [9] A. Tankus, Y. Yeshurun, and N. Intrator. Face detection by direct convexity estimation. *Pattern Recognition Letters*, 18:913–922, 1997.
- [10] I. V. Ternovskiy and T. Jansson. Mapping-singularities-based motion estimation. *Proc. SPIE*, 3173:317–321, 1997.
- [11] A. H. Thayer. An arraignment of the theories of mimicry and warning colours. *Popular Science Monthly, N.Y.*, pages 550–570, 1909.